

# Relaxing Constraints on Inflation Models with Curvaton

Takeo Moroi<sup>a</sup>, Tomo Takahashi<sup>b</sup> and Yoshikazu Toyoda<sup>a</sup>

<sup>a</sup>*Department of Physics, Tohoku University  
Sendai 980-8587, Japan*

<sup>b</sup>*Institute for Cosmic Ray Research, University of Tokyo  
Kashiwa 277-8582, Japan*

## Abstract

We consider the effects of the curvaton, late-decaying scalar condensation, to observational constraints on inflation models. From current observations of cosmic density fluctuations, severe constraints on some class of inflation models are obtained, in particular, on the chaotic inflation with higher-power monomials, the natural inflation, and the new inflation. We study how the curvaton scenario changes (and relaxes) the constraints on these models.

# 1 Introduction

Inflation, a superluminal expansion at the early stage of the universe [1], is one of the most promising ideas to solve the flatness and horizon problems which are serious drawbacks of the standard hot big bang model. Inflation can be caused by the potential energy of a scalar field called inflaton which slowly rolls down the potential. Since quantum fluctuation of the inflaton during inflation is usually assumed to be the origin of cosmic density perturbation, models of inflation can be tested by observations of cosmic microwave background (CMB), large scale structure and so on. Recent results from Wilkinson microwave anisotropy probe (WMAP) [2] gave severe constraints on inflation models [3]. For example, chaotic inflation model [4] with quartic potential  $V_{\text{inf}} \propto \chi^4$ , where  $\chi$  is the inflaton, is on verge of exclusion by observations assuming the standard thermal history of the universe.

However today's cosmic fluctuation can originate to some source other than the inflaton. In the curvaton scenario [5], adiabatic fluctuation can be given by primordial fluctuation of some late-decaying scalar field which is called curvaton. In this scenario, the superluminal expansion is caused by the inflaton while (some part of) the fluctuation responsible for the cosmic fluctuation today is provided by the curvaton field. Thus, in this case, constraints on models of inflation can be alleviated to some extent. Even if the fluctuation of the inflaton is partly relevant to the today's fluctuation, we can expect that constraints on models of inflation can be relaxed compared to the case without the curvaton. The authors of Ref. [6] studied the constraint on the quartic chaotic inflation model in the curvaton scenario and showed that the quartic chaotic inflation model is still viable in the curvaton scenario.

In this paper, we investigate this issue in detail for various inflation models which, in particular are on verge or already excluded in the standard inflationary scenario. We will show that some inflation models can be made viable in the curvaton scenario.

The organization of this paper is as follows. In the next section, we give a brief review of the scenario where both inflaton and curvaton fluctuations give today's cosmic fluctuations and define our notations. In addition, we also describe our analysis method. In Section 3, we discuss to what extent constraints on inflation models are alleviated in the curvaton scenario starting from the chaotic inflation model, the natural inflation model and the new inflation model. The conclusion of our study is given in the final section.

## 2 Formalism

### 2.1 Background Evolution

The aim of this paper is to investigate to what extent constraints on inflation models can be relaxed in the curvaton scenario. Thus we need to discuss density perturbations. However, before discussing density perturbations, first we discuss the background evolution and fix our notations.

We start with the inflationary era. During inflation, there assumed to be two scalar fields, one is the inflaton  $\chi$  and the other is the curvaton  $\phi$  which follow the following equations of motion;

$$\ddot{\chi} + 3H\dot{\chi} + \frac{dV_{\text{inf}}}{d\chi} = 0, \quad (2.1)$$

$$\ddot{\phi} + 3H\dot{\phi} + \frac{dV_{\text{curv}}}{d\phi} = 0, \quad (2.2)$$

where the dot represents derivative with respect to time,  $V_{\text{inf}}$  and  $V_{\text{curv}}$  are the potentials for the inflaton and the curvaton, respectively.  $H$  is the Hubble parameter which is given by

$$H^2 = \left(\frac{\dot{a}}{a}\right)^2 = \frac{1}{3M_{\text{pl}}^2}\rho_{\text{tot}}, \quad (2.3)$$

where  $a$  is the scale factor,  $M_{\text{pl}} \simeq 2.4 \times 10^{18}$  GeV is the reduced Planck scale, and  $\rho_{\text{tot}}$  the total energy density of the universe. During inflation, it is given by the sum of contributions from the inflaton and the curvaton as

$$\rho_{\text{tot}} = \rho_{\chi} + \rho_{\phi} = \frac{1}{2}\dot{\chi}^2 + V_{\text{inf}} + \frac{1}{2}\dot{\phi}^2 + V_{\text{curv}}. \quad (2.4)$$

For the potential of the inflaton, we consider various possibilities which we will describe later. For the curvaton, for simplicity, we consider the quadratic potential in this paper;

$$V(\phi) = \frac{1}{2}m_{\phi}^2\phi^2, \quad (2.5)$$

where  $m_{\phi}$  is the mass of the curvaton.

After the inflation, the inflaton begins to oscillate around the minimum of the potential. We call this epoch as  $\chi$ -dominated or  $\chi$ D era. Then, the inflaton decays when  $H \sim \Gamma_{\chi}$  (with  $\Gamma_{\chi}$  being the decay rate of the inflaton). In this period, the evolution of the inflaton is described by Eq. (2.1) with the decay term being included. Once the expansion rate  $H$  becomes much smaller than the oscillation frequency of  $\chi$ , however, it is rather convenient to consider the averaged value of the energy density of  $\chi$  and to follow its evolution. Indeed, for the inflaton potential  $V_{\text{inf}} \propto \chi^n$ ,  $\rho_{\chi}$  follows the equation

$$\dot{\rho}_{\chi} = -3(1 + w_{\chi})H\rho_{\chi} - \Gamma_{\chi}\rho_{\chi}, \quad (2.6)$$

with  $w_{\chi} = (n - 2)/(n + 2)$ . Thus, the energy density of the oscillating inflaton behaves as [7]

$$\rho_{\chi} \propto a^{-\frac{6n}{n+2}}. \quad (2.7)$$

In our study, we only consider the case where  $\Gamma_{\chi}$  is small enough so that the inflaton decays when  $H$  is much smaller than the oscillation frequency of  $\chi$ . Thus, the reheating

processes by the inflaton is studied by using Eq. (2.6). In addition, the energy density of the radiation evolves as

$$\dot{\rho}_{\text{rad}} = -4H\rho_{\text{rad}} + \Gamma_{\chi}\rho_{\chi} + \Gamma_{\phi}\rho_{\phi}, \quad (2.8)$$

with  $\Gamma_{\phi}$  being the decay rate of the curvaton. Here, we included the effect of the curvaton decay, which will become important in the following discussion. When  $H \sim \Gamma_{\chi}$ , the inflaton decays into radiation, then the universe is reheated to become radiation-dominated. We call this radiation dominated era “RD1.”

When the expansion rate of the universe becomes comparable to  $m_{\phi}$ , the curvaton also starts to oscillate, then it behaves like matter component for the potential given in Eq. (2.5). Thus, at some epoch the universe becomes curvaton dominated. We call this epoch “ $\phi$ D” era. After the  $\phi$ D era, the curvaton decays into radiation then the universe becomes radiation dominated again. We call this epoch “RD2” era. The time when the RD2 era starts depends on the decay rate of the curvaton  $\Gamma_{\phi}$ . From  $\phi$ D era to RD2 era, the universe consists of radiation and the oscillating curvaton field. Since the curvaton behaves like matter in this epoch, energy density of the curvaton is governed by the following equation

$$\dot{\rho}_{\phi} = -3H\rho_{\phi} - \Gamma_{\phi}\rho_{\phi}. \quad (2.9)$$

When the initial amplitude of the curvaton is as large as  $\phi_{\text{init}} \sim M_{\text{pl}}$ , the curvaton can cause the second inflation after the usual inflation provided by the inflaton. In this case, the second inflation epoch exists before  $\phi$ D era mentioned above. Depending on the initial amplitude and mass of the curvaton, the second inflation era can start during  $\chi$ D era or RD1 era. Such effect is also taken into account in our analysis (in particular, in our numerical study to evaluate the  $e$ -folding number during the inflation).

Here we summarize what we need to fix the background evolution. As for the background, the following parameters are necessary to determine the thermal history of the universe except the potential of the inflaton (and the initial amplitude of the inflaton): the mass of the curvaton  $m_{\phi}$ , the initial amplitude of the curvaton  $\phi_{\text{init}}$ , the decay rates of the inflaton and the curvaton  $\Gamma_{\chi}$  and  $\Gamma_{\phi}$ .

## 2.2 Density Perturbation

Next we discuss the density perturbation in the scenario. Since there are two sources of cosmic density fluctuation in this case (i.e., the inflaton and the curvaton), we need to take account of the effects of both of them. Since the primordial fluctuations of the inflaton and the curvaton are uncorrelated, we can study their effects separately. First we summarize the results for the standard case, i.e., the case with the inflaton only. Then we will discuss how the situation is modified in the curvaton scenario.

The quantum fluctuation of the inflaton  $\delta\chi$  during inflation generates the curvature perturbation as  $\mathcal{R} = -(H/\dot{\chi})\delta\chi$ . Since  $\delta\chi \simeq H/2\pi$ , the power spectrum of the curvature

perturbation from the inflaton fluctuation is

$$P_{\mathcal{R}}^{(\text{inf})} = \frac{1}{12\pi^2 M_{\text{pl}}^6} \left. \frac{V_{\text{inf}}^3}{V_{\text{inf}}'^2} \right|_{k=aH}, \quad (2.10)$$

where the “prime” is the derivative with respect to  $\chi$ . Here, we used the slow-roll approximation. To discuss observational consequences, we have to set up the initial condition during radiation dominated era after the decay of the inflaton. For this purpose, we represent the primordial power spectrum with the (Bardeen’s) gravitational potential  $\Phi$  which appears in the perturbed metric in the conformal Newtonian (or longitudinal) gauge as

$$ds^2 = -a^2(1 + 2\Phi)d\tau^2 + a^2(1 - 2\Psi)dx^2, \quad (2.11)$$

with  $\tau$  being the conformal time. During radiation-dominated era,  $\Phi$  and  $\mathcal{R}$  are related as  $\Phi = -(2/3)\mathcal{R}$ . Thus the power spectrum of  $\Phi$  is given by  $P_{\Phi} = (4/9)P_{\mathcal{R}}$ . The spectral index of the primordial power spectrum is

$$n_s - 1 \equiv \frac{d \ln P_{\Phi}}{d \ln k}. \quad (2.12)$$

Using the slow-roll parameters defined as<sup>#1</sup>

$$\epsilon \equiv \frac{1}{2} M_{\text{pl}}^2 \left( \frac{V_{\text{inf}}'}{V_{\text{inf}}} \right)^2, \quad \eta \equiv M_{\text{pl}}^2 \frac{V_{\text{inf}}''}{V_{\text{inf}}}, \quad (2.13)$$

the spectral index can be written as

$$n_s^{(\text{inf})} - 1 = -6\epsilon + 2\eta. \quad (2.14)$$

During inflation, the gravity wave can also be generated. The primordial gravity wave (tensor) power spectrum is given by

$$P_T^{(\text{inf})} = \frac{2V_{\text{inf}}}{3\pi^2 M_{\text{pl}}^4}. \quad (2.15)$$

With this expression, the tensor-scalar ratio  $r$  is defined and given by

$$r^{(\text{inf})} \equiv \frac{P_T^{(\text{inf})}}{P_{\mathcal{R}}^{(\text{inf})}} = \frac{4}{9} \frac{P_T^{(\text{inf})}}{P_{\Phi}^{(\text{inf})}} = 16\epsilon. \quad (2.16)$$

Now, we consider the fluctuations generated by the curvaton fluctuation. Let us start with summarizing the equations relevant for the following discussion. From the Einstein equation, we obtain the perturbation equation for the metric perturbations:

$$-k^2\Phi = \frac{3}{2}\mathcal{H}^2 \left[ \delta_{\text{tot}} + \frac{3\mathcal{H}}{k}(1 + \omega_{\text{tot}})V_{\text{tot}} \right], \quad (2.17)$$

---

<sup>#1</sup>In this paper, we use so-called “potential” slow-roll parameters which are defined using the value of the potential not using the Hubble parameter.

where  $\mathcal{H} = (1/a)(da/d\tau)$  is the conformal Hubble parameter,  $\delta_X = \delta\rho_X/\rho_X$  and  $V_X$  are density perturbation and velocity perturbation of a component  $X$ . In the above equation, “tot” denotes the total matter, and  $w_{\text{tot}} = p_{\text{tot}}/\rho_{\text{tot}}$  is the equation-of-state parameter of the total matter. Assuming that the anisotropic stress is negligible, the metric perturbation variables are related as  $\Phi = \Psi$ . The equations for the density and velocity perturbations of the component whose equation-of-state parameter is  $\omega_X$  are

$$\frac{d\delta_X}{d\tau} = -(1 + \omega_X) \left( kV_X - 3\frac{d\Psi}{d\tau} \right), \quad (2.18)$$

$$\frac{dV_X}{d\tau} = -\mathcal{H}(1 - 3\omega_X)V_X + \frac{\omega_X}{1 + \omega_X}k\delta_X + k\Phi. \quad (2.19)$$

Evolutions of the fluctuations are followed by solving the above equations (as well as those for the background quantities). Since there are two independent contributions to the cosmic density fluctuations, i.e., the primordial fluctuations of the inflaton and the curvaton,  $\Phi_{\text{RD2}}$  in this case has two terms which are proportional to  $\delta\chi_{\text{init}}$  and  $\delta\phi_{\text{init}}$ , respectively:

$$\Phi_{\text{RD2}} = -\frac{2}{3M_{\text{pl}}^2} \frac{V_{\text{inf}}}{V'_{\text{inf}}} \delta\chi_{\text{init}} - f(X) \frac{\delta\phi_{\text{init}}}{M_{\text{pl}}}, \quad (2.20)$$

where  $\delta\phi_{\text{init}}$  is the primordial fluctuation of the curvaton, and

$$X = \frac{\phi_{\text{init}}}{M_{\text{pl}}}. \quad (2.21)$$

The first term of the right-hand side of Eq. (2.20) is the inflaton contribution which we have already discussed before. The second term is the curvaton contribution; in our study,  $f(X)$  is calculated by numerically solving the Einstein and Boltzmann equations. Here, the curvaton contribution is parameterized by the function  $f(X)$  [6]. Although we have used the numerical method to calculate  $f(X)$ , effects of the curvaton can be easily evaluated for the cases where the initial amplitude of the curvaton is much larger or much smaller than  $M_{\text{pl}}$  [6, 8]. Indeed, for these cases,  $f(X)$  is given by

$$f(X) \simeq \begin{cases} \frac{4}{9X} & : \phi_{\text{init}} \ll M_{\text{pl}} \\ \frac{1}{3}X & : \phi_{\text{init}} \gg M_{\text{pl}} \end{cases}. \quad (2.22)$$

Assuming that the inflaton and the curvaton are uncorrelated, we find the power spectrum of  $\Phi$  as [6]

$$P_{\Phi} = \left[ 1 + \tilde{f}^2(X)\epsilon \right] \frac{V_{\text{inf}}}{54\pi^2 M_{\text{pl}}^4 \epsilon}, \quad (2.23)$$

where  $\tilde{f} = (3/\sqrt{2})f$ . The scalar spectral index is given by using Eq. (2.14)

$$n_s - 1 = -2\epsilon + \frac{2\eta - 4\epsilon}{1 + \tilde{f}^2\epsilon}. \quad (2.24)$$

The tensor power spectrum is not modified even with the curvaton. However, since the scalar perturbation spectrum is modified, the tensor-scalar ratio becomes

$$r = \frac{16\epsilon}{1 + \tilde{f}^2\epsilon}. \quad (2.25)$$

### 3 Results

Now, we are ready to discuss how the constraints on inflation models are alleviated with curvaton. We investigate the following inflation models; chaotic inflation models for several monomials, the natural inflation model and the new inflation model. For these models, observations of CMB anisotropy and large scale structure provide severe constraints and some part of the parameter space in these models is excluded in the standard scenarios.

Including the curvaton contributions, we analyze the constraints on these inflation models, making use of the observational constraints on the scalar spectral index  $n_s$  and the tensor-scalar ratio  $r$ . In our analysis, we first calculate  $n_s$  and  $r$  for a given model. For this purpose, it is important to determine the amplitude of the inflaton field at the time of the horizon exit  $\chi_*$ ; once  $\chi_*$  is given,  $n_s$  and  $r$  are calculated by using Eqs. (2.24) and (2.25). (In this paper, the subscript “\*” is used for the quantities at the time of the horizon exit.) Importantly,  $\chi_*$  depends on various parameters. In order for the systematic and precise determination of  $\chi_*$ , we followed the evolution of the inflaton and the curvaton field (as well as the energy density of radiation) from the inflationary era to the RD2 era by numerically solving the Einstein and Boltzmann equations given in the previous section. Since we evaluate the values of  $n_s$  and  $r$  at  $k = 0.01\text{Mpc}^{-1}$  to compare a model with observations of CMB and large scale structure,  $\chi_*$  is determined by the condition  $H_*(a_*/a_0) = 0.01\text{Mpc}^{-1}$ , where  $a_*$  and  $H_*$  are the scale factor and the expansion rate at  $\chi = \chi_*$ , respectively, and  $a_0$  is the present scale factor. In our analysis,  $\chi_*$  is calculated as a function of  $X$ ,  $m_\phi$ , and other model parameters (in particular, the decay rates of the inflaton and curvaton). With  $\chi_*$ , we calculate  $n_s$  and  $r$ .<sup>#2</sup> Then, we compare them with the observational constraints on  $n_s$  and  $r$  obtained by many authors (see e.g., [9]). In our analysis, allowed region on the  $m_\phi$  vs.  $X$  plane is given by the region where  $(n_s, r)$  calculated with  $(X, m_\phi)$  falls onto the 95 % C.L. allowed region on the  $n_s$  vs.  $r$  plane given in Ref. [9]. In the cases of the natural inflation and the new inflation, we show the constraints in other planes instead of the  $m_\phi$  vs.  $X$  plane replacing  $m_\phi$  with another parameter in the inflaton sector. However, even in such a case, the analysis method is the same as above.

---

<sup>#2</sup>Strictly speaking, as for CMB data, we have to compare the data with  $C_l = C_l^{(\delta\chi)} + C_l^{(\delta\phi)}$  where  $C_l^{(\delta\chi)}$  and  $C_l^{(\delta\phi)}$  are contributions from the primordial fluctuation of the inflaton and the curvaton, respectively, and similarly for observations of large scale structure. We checked that calculations of  $C_l$  using of the effective spectral index does not affect our results (the final  $C_l$  does not change within 0.1 % error). Thus, for the purpose of this paper, we can use the effective spectral index in our analysis.

### 3.1 Chaotic Inflation

We parameterize the potential for the chaotic inflation as

$$V_{\text{inf}} = \lambda M_{\text{pl}}^4 \left( \frac{\chi}{M_{\text{pl}}} \right)^\alpha. \quad (3.1)$$

Here, we require  $\alpha$  to be an even integer for the positivity and smoothness of the inflaton potential. We consider the cases with  $\alpha \geq 4$ , for which observations of CMB and large scale structure provide severe constraints for the case without the curvaton.

The slow-roll parameters in this model are given by

$$\epsilon = \frac{1}{2} \alpha^2 \frac{M_{\text{pl}}^2}{\chi_*^2}, \quad \eta = \alpha(\alpha - 1) \frac{M_{\text{pl}}^2}{\chi_*^2}. \quad (3.2)$$

The moment when the present horizon scale exits the horizon during inflation is usually denoted with the  $e$ -folding number of inflation which is defined as the logarithm of the ratio of the scale factors at the horizon crossing and the end of inflation:  $N_e \equiv \ln(a_*/a_{\text{end}})$ . We can write this quantity with the amplitude of the inflaton

$$N_e = \frac{1}{M_{\text{pl}}^2} \int_{\chi_{\text{end}}}^{\chi_*} \frac{V_{\text{inf}}}{V'_{\text{inf}}} d\chi, \quad (3.3)$$

where  $\chi_{\text{end}}$  is determined as the inflaton amplitude when one of the slow-roll parameters becomes 1.

Since the amplitude of the inflaton at the end of inflation is much smaller than  $\chi_*$ , the  $e$ -folding number can be written as

$$N_e \simeq \frac{1}{2\alpha M_{\text{pl}}^2} \chi_*^2. \quad (3.4)$$

Although  $N_e$  depends on the thermal history of the universe, it is often assumed that  $N_e \sim 50$ . If we take  $N_e = 50$ , the scalar spectral index and the tensor-scalar ratio  $(n_s - 1, r)$  are  $(-0.06, 0.32)$  for  $\alpha = 4$ , which are marginally excluded by the WMAP result. For  $\alpha = 6$  and 8,  $(n_s - 1, r) = (-0.08, 0.48)$  and  $(-0.1, 0.64)$ , respectively, which are completely ruled out.

However, in the curvaton scenario, fluctuation of the curvaton also affects the primordial spectrum. As for the spectral index, we can see from Eq. (2.24) that  $n_s$  becomes smaller in the case with curvaton. The tensor-scalar ratio also becomes smaller as we can see from Eq. (2.25). Thus constraints on the inflation models based on  $n_s$  and  $r$  can be relaxed with curvaton. However, notice that, in the curvaton scenario, the background evolution is also changed. In particular, when the second inflation occurs, it may decrease the  $e$ -foldings during the first inflation by 20 – 30. Thus  $N_e$  during inflation changes depending on the parameters of the curvaton such as mass, initial amplitude and decay rate. (Of course it depends on the inflaton parameters such as the decay rate of the inflaton.) This also changes the constraints on inflation models. Details of the change will be discussed for each models.



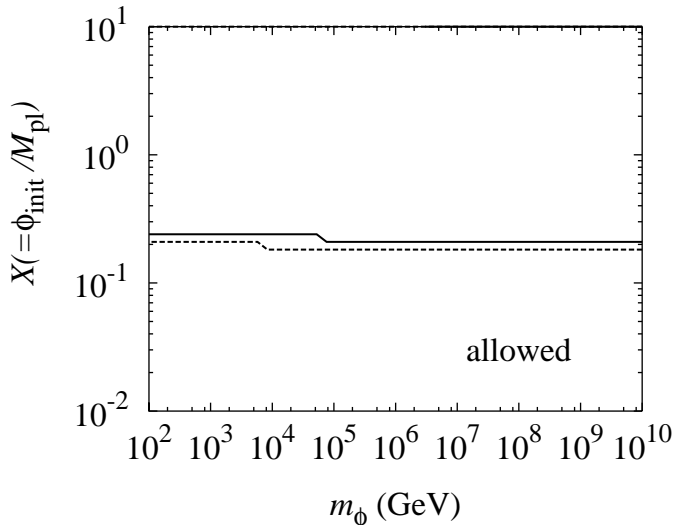


Figure 1: The 95 % C.L. allowed regions are shown for  $\alpha = 4$ . The decay rate of the curvaton is assumed to be  $\Gamma_\phi = 10^{-18}$  GeV (solid line) and  $\Gamma_\phi = 10^{-10}$  GeV (dashed line). Lower side of the horizontal line is allowed for the given  $\Gamma_\phi$ .

### 3.1.1 $\alpha = 4$ case

The chaotic inflation with  $\alpha = 4$  is on verge of exclusion by cosmological observations as mentioned above. Here we consider how this constraint changes in the curvaton scenario.

First we describe how we treat free parameters in this model. The free parameters in this model are the coupling in the potential  $\lambda$ , the mass of the curvaton  $m_\phi$ , the initial amplitude of the curvaton  $\phi_{\text{init}}$  and the decay rate of the curvaton  $\Gamma_\phi$ . Although the decay rate of the inflaton also affect the number of  $e$ -foldings in general, oscillating inflaton field in this model behaves as radiation, namely the energy density of the oscillating scalar field is given by  $\rho_\chi \propto a^{-4}$ . Hence  $\Gamma_\chi$  is irrelevant to determine the number of  $e$ -foldings in this model. For the coupling parameter  $\lambda$ , it can be fixed to have right amount of density fluctuation. However, the scalar spectral index and the tensor-scalar ratio are independent of  $\lambda$ , as we can see from Eq. (2.24). Since we discriminate the model using the constraints on  $n_s$  and  $r$ , we do not discuss  $\lambda$  in the following.

In Fig. 1, the 95 % C.L. allowed regions are shown for some values of  $\Gamma_\phi$  in the  $m_\phi$  vs.  $X$

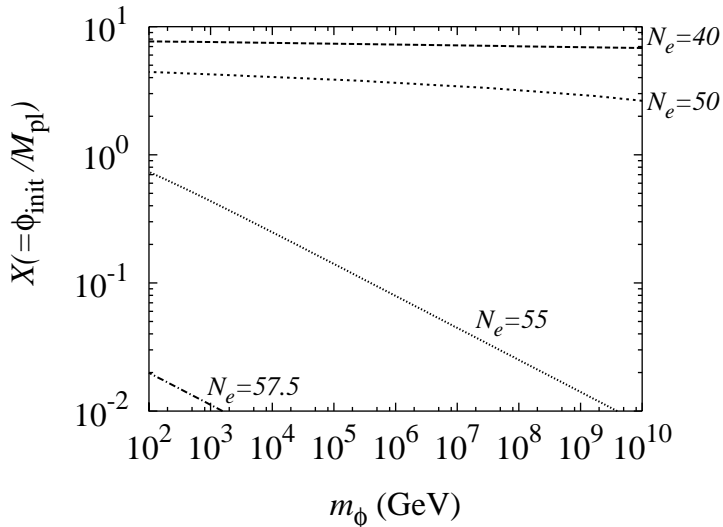


Figure 2: Contours of constant  $N_e$  during inflation for the case with  $\alpha = 4$ . The decay rate of the curvaton is assumed to be  $\Gamma_\phi = 10^{-10}$  GeV.

plane. As discussed in the previous section, contribution from the curvaton fluctuation to the adiabatic fluctuation becomes large for small  $\phi_{\text{init}}$ , thus regions with small  $X$  become allowed. On the other hand, regions with large initial amplitude are excluded for most cases. In fact, in such region, the contributions from the curvaton fluctuation becomes large. However, with such large initial amplitude, the second inflation happens with the energy density of the curvaton. Accordingly the number of  $e$ -foldings during the first inflation becomes smaller. In Fig. 2, we show contours of constant number of  $e$ -foldings in this model. We can see that regions with large  $X$  give small number of  $e$ -foldings. Thus the amplitude of inflaton at the horizon crossing becomes smaller than that of usual cases. This is the reason why regions with large  $X$  cannot alleviate the inflation model even though the contribution to the curvature perturbation from the fluctuation of the curvaton is large there.

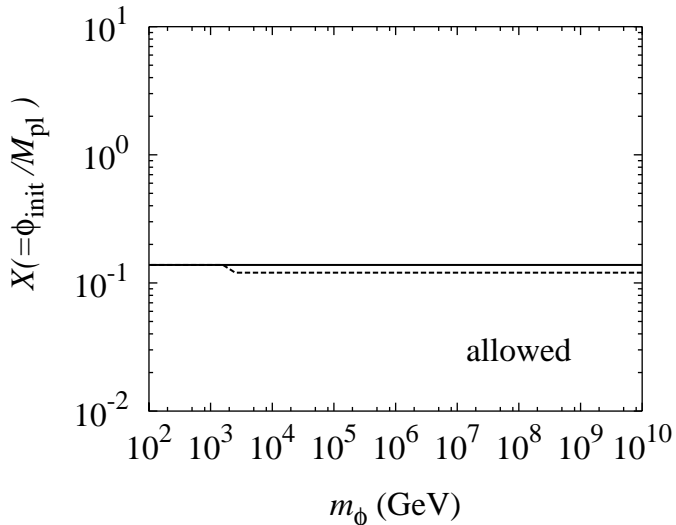


Figure 3: The 95 % C.L. allowed regions for  $\alpha = 6$ . The decay rate of the inflaton is taken to be  $\Gamma_\chi = 10^8$  GeV. The decay rate of the curvaton is assumed to be  $\Gamma_\phi = 10^{-18}$  GeV (solid line) and  $\Gamma_\phi = 10^{-10}$  GeV (dashed line). The lower side of the horizontal line is allowed for the given  $\Gamma_\chi$ .

### 3.1.2 $\alpha \geq 6$ case

Next we discuss the case with  $\alpha = 6$ . The situation is very similar to the case with  $\alpha = 4$ . One of differences is that, once the inflaton starts to oscillate, its energy density evolves as  $\rho_\chi \propto a^{-4.5}$  which is stiffer than that of radiation. Thus the constraint on the  $m_\phi$  vs.  $X$  plane depends on the decay rate of the inflaton in this case. We present the results for  $\Gamma_\chi = 10^8$  GeV and  $10^6$  GeV in Figs. 3 and 4, respectively. Similarly to the case with  $\alpha = 4$ , regions with small  $X$  can relax the constraints on the inflation model.

So far, we have seen that, for  $\alpha = 4$  and 6, the chaotic inflation models become viable when the initial amplitude of the curvaton is small enough. As one can expect, similar results are obtained for larger values of  $\alpha$ . We have calculated the upper bounds on  $X$  which make the chaotic inflation models with  $\alpha \geq 6$  viable. The bound is given by  $X \leq 0.137$  (0.088) for  $\alpha = 6$  (8). Here, we have taken  $\Gamma_\chi = 10^6$  GeV,  $m_\phi = 10^2$  GeV and  $\Gamma_\phi = 10^{-10}$  GeV.

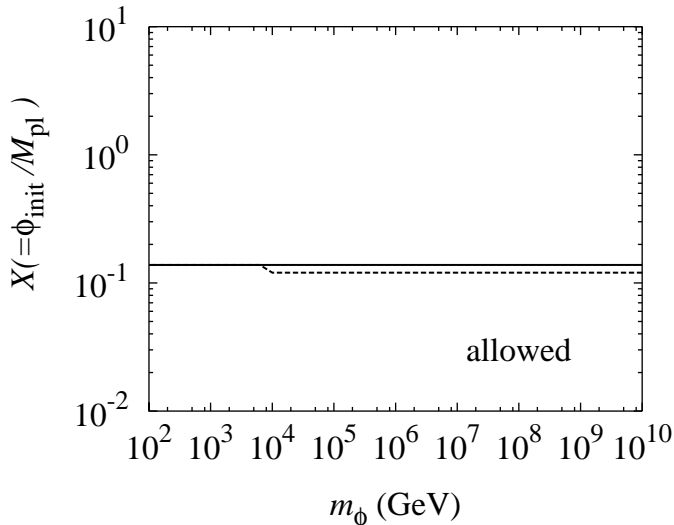


Figure 4: Same as Fig. 3, except for  $\Gamma_\chi = 10^6$  GeV.

Since the model with larger values of  $\alpha$  predicts smaller  $n_s - 1$ , upper bound on  $X$  becomes severer for larger value of  $\alpha$ . In particular, with the decay rates and the curvaton mass used above, models with  $\alpha \geq 10$  cannot become viable even with the curvaton. This is because, even if the curvaton contribution dominates, the spectral index  $n_s \simeq 1 - 2\epsilon \simeq 1 - \alpha/2N_e$  becomes too small to be consistent with the observations. For  $\alpha = 10$ , for example,  $n_s - 1 \simeq -0.1$  with  $N_e \simeq 50$ , which is excluded by the observations. One possibility to make the models with large  $\alpha$  viable is to increase the  $e$ -folding number  $N_e$  since  $n_s - 1$  is approximately proportional to  $N_e^{-1}$  in this case. Larger value of  $N_e$  is realized with, for example, smaller value of  $\Gamma_\chi$  or larger value of  $\Gamma_\phi$ .

### 3.2 Natural Inflation

The natural inflation model [10, 11] is based on a (psuedo-)Nambu-Goldstone (NG) field which has a potential of the form

$$V_{\text{inf}} = \Lambda^4 \left[ 1 - \cos \left( \frac{\chi}{F} \right) \right]. \quad (3.5)$$

In this case, the slow-roll parameters are given by

$$\epsilon = \frac{1}{2} \left( \frac{M_{\text{pl}}}{F} \right)^2 \frac{1}{\tan^2(\chi/2F)}, \quad \eta = \frac{1}{2} \left( \frac{M_{\text{pl}}}{F} \right)^2 \left[ \frac{1}{\tan^2(\chi/2F)} - 1 \right]. \quad (3.6)$$

The inflation ends when the slow-roll condition does not hold, namely one of the slow-roll parameters becomes  $\mathcal{O}(1)$ . The amplitude of the inflaton at the end of inflation can be obtained by

$$\tan \left( \frac{\chi_{\text{end}}}{2F} \right) \simeq \frac{M_{\text{pl}}}{\sqrt{2}F}. \quad (3.7)$$

The number of  $e$ -folding can be evaluated using the standard technique as

$$N_e = \frac{2F^2}{M_{\text{pl}}^2} \ln \left[ \frac{\cos(\chi_{\text{end}}/2F)}{\cos(\chi_*/2F)} \right] \quad (3.8)$$

After the inflation, the inflaton starts to oscillate around the minimum of the potential. Around the minimum, the potential can be well-approximated as a quadratic form  $V_{\text{inf}} \simeq (1/2)(\Lambda^2/F)^2\chi^2$ . Thus the energy density of oscillating inflaton field behaves as the same as that of matter. The natural inflation model generally predicts a red-tilted primordial spectrum and small tensor-scalar ratio [12]. However, in the curvaton scenario, the spectral index can approach to the scale-invariant value, which can alleviate the constraint on this model. The modification can be obtained using the formulae given in the previous section.

In Fig. 5, the 95 % allowed regions are shown in the  $F$  vs.  $X$  plane. In the figure, the values of  $\Lambda$  are chosen to give a minimal value of  $\chi^2$  from WMAP data using the code provided by them [13]. In principle, the constraint also depends on the mass of the curvaton. However, since we checked that the variation of the mass of the curvaton does not affect the constraint much, we only show the result on the  $F$  vs.  $X$  plane.

When fluctuation of the curvaton has a small contribution to the total curvature fluctuation, the spectral index is too small to be consistent with the observations in the natural inflation model. However, as same as the case with the chaotic inflation models, larger contribution from the curvaton fluctuation can liberate the model. In particular, the natural inflation predicts smaller spectral index as  $F$  decreases. Correspondingly, the upper limit on  $X$  where the curvaton mechanism can liberate the model becomes smaller as it can be seen from Fig. 5.

### 3.3 New Inflation

Among various possibilities of the new inflation models, we chose to use the one proposed in [14, 15] to be definite. The model is based on the supersymmetric models with  $Z_n$   $R$ -symmetry. We parameterize the superpotential with the parameters  $\lambda$  and  $v$  as

$$W = \frac{\lambda}{v^{n-2}} \left( v^n \hat{\chi} - \frac{1}{n+1} \hat{\chi}^{n+1} \right), \quad (3.9)$$

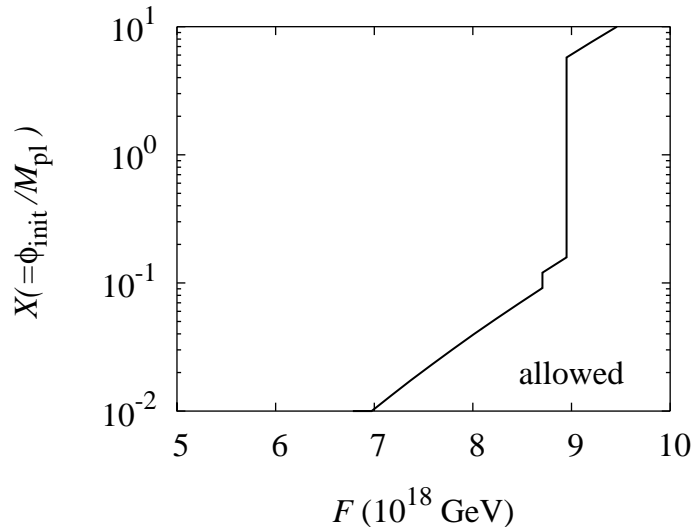


Figure 5: The 95 % C.L. allowed regions are shown for the natural inflation model in the  $F$  vs.  $X$  plane. The lower region under the line is allowed. The decay rate of the inflaton and the curvaton are assumed to be  $\Gamma_\chi = 10^6$  GeV and  $10^{-10}$  GeV, respectively in this figure. The mass of the curvaton is  $m_\phi = 10^2$  GeV.

where  $\hat{\chi}$  is the superfield for the inflaton.

Using the fact that the inflaton  $\chi$  is a real scalar field, the inflaton potential is given by<sup>#3</sup>

$$V_{\text{inf}} = \tilde{\lambda}^2 \tilde{v}^4 \left[ 1 - 2 \left( \frac{\chi}{\tilde{v}} \right)^n + \left( \frac{\chi}{\tilde{v}} \right)^{2n} \right], \quad (3.10)$$

---

<sup>#3</sup>In supergravity, extra term may arise in the inflaton potential with non-minimal Kähler potential. We assume that the higher-order terms in the Kähler potential are small enough to be neglected. It is the case in, for example, the class of models with large cutoff scale [16]. In addition, if we naively use the superpotential given in Eq. (3.9) in supergravity, negative cosmological constant arises at the minimum of the potential. We assume that the cosmological constant problem is somehow solved since it is not our main issue. Thus, we assume that the inflaton potential can be well approximated by Eq. (3.10) even near the minimum of the potential.

with

$$\tilde{\lambda} = \frac{1}{2}\lambda, \quad \tilde{v} = \sqrt{2}v. \quad (3.11)$$

Here, we neglect the higher order terms which are allowed by the  $Z_n$  symmetry. Assuming that the higher-order terms are suppressed by the inverse powers of the Planck scale, the scalar potential given above is relevant when  $\tilde{v} \ll M_{\text{pl}}$ . In the following, we first analyze the model using the above superpotential, allowing the  $v$  parameter to be as large as  $M_{\text{pl}}$ . After deriving the constraints, we take account of the constraint  $\tilde{v} \ll M_{\text{pl}}$  and discuss the implications.

In this model, for a given value of  $\tilde{v}$ , the  $\tilde{\lambda}$  parameter is determined so that the cosmic density fluctuation have the correct size. However, as we see below, the spectral index and the tensor-scalar ratio are independent of  $\tilde{\lambda}$ .

Now we evaluate the slow-roll parameters in the model. During inflation, the last term in Eq. (3.10) is irrelevant to the dynamics of the inflaton. Thus we neglect the last term for the moment. The slow-roll parameters are

$$\epsilon = 2n^2 \left( \frac{M_{\text{pl}}}{\tilde{v}} \right)^2 \left( \frac{\chi_*}{\tilde{v}} \right)^{2(n-1)}, \quad \eta = -2n(n-1) \left( \frac{M_{\text{pl}}}{\tilde{v}} \right)^2 \left( \frac{\chi_*}{\tilde{v}} \right)^{n-2}. \quad (3.12)$$

The number of  $e$ -folding is given as

$$N_e = \frac{1}{2n(n-2)} \left( \frac{\tilde{v}}{M_{\text{pl}}} \right)^2 \left( \frac{\chi_*}{\tilde{v}} \right)^{n-2}. \quad (3.13)$$

Thus, in the standard inflationary scenario, the scalar spectral index can be written as

$$n_s - 1 = -2 \frac{n-1}{n-2} \frac{1}{N_e}. \quad (3.14)$$

For  $N_e = 50$ , for example,  $n_s - 1$  becomes  $-0.08$ ,  $-0.06$  and  $-0.053$  for  $n = 3, 4$  and  $5$ , respectively. In particular, the model with  $n = 3$  is marginally excluded by observations.

The situation for  $n = 3$  may be improved by the curvaton, as before. In Fig. 6, we plot the 95 % C.L. allowed region in the  $v$  vs.  $X$  plane. Notice that this model predicts very small value of the  $\epsilon$  parameter, in particular for the case with  $\tilde{v} \ll M_{\text{pl}}$ . Using the  $e$ -folding number and the amplitude of the inflaton at the horizon crossing,  $\epsilon$  is given as

$$\epsilon = 2n^2 \left( \frac{M_{\text{pl}}}{\tilde{v}} \right)^2 \left[ \frac{1}{2n(n-2)} \left( \frac{\tilde{v}}{M_{\text{pl}}} \right)^2 \frac{1}{N_e} \right]^{\frac{2(n-1)}{n-2}}. \quad (3.15)$$

For  $n = 3$ , this equation becomes  $\epsilon = 18(1/6N)^4(\tilde{v}/M_{\text{pl}})^6$ . For  $N_e = 50$  and  $\tilde{v} \sim 10^{16}$  GeV, for example, the  $\epsilon$  parameter becomes of order  $10^{-21}$ . Importantly, the effects of the curvaton comes in the combination  $\tilde{f}^2\epsilon$  in the formula of the scalar spectral index (see Eq.

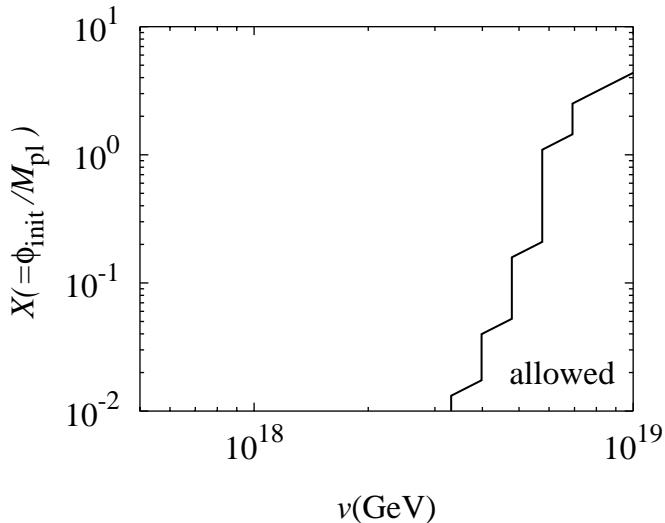


Figure 6: The 95 % C.L. allowed region is shown for the natural inflation model in the  $v$  vs.  $X$  plane. The lower region under the line is allowed. The decay rate of the inflaton and the curvaton are assumed to be  $\Gamma_\chi = 10^6$  GeV and  $10^{-10}$  GeV, respectively in this figure. The mass of the curvaton is  $m_\phi = 10^2$  GeV.

(2.24)). Thus, the curvaton can help to flatten the primordial scalar power spectrum only when  $\tilde{v}$  is large enough.

As we mentioned before, the new inflation model based on the  $Z_n$   $R$ -symmetry requires  $v \ll M_{\text{pl}}$  [14, 15]. In this case, the  $\epsilon$  parameter is always very small and the curvaton contribution is always suppressed. Thus, it is difficult to make the (supersymmetric) new inflation model based on  $Z_n$   $R$ -symmetry viable with the curvaton mechanism.

## 4 Conclusion

In this paper, we have studied the constraints on the inflaton potential taking account of the effects of the curvaton. We have followed the basic procedure given in Ref. [6]. We have considered several models of the inflation for which some part of the parameter space is excluded by the observations. We have seen that the constraints on these models can



be relaxed once the curvaton is introduced.

For the case of the chaotic inflation, inflation models with the inflaton potential  $V_{\text{inf}} \propto \chi^\alpha$  can become viable with curvaton, if  $\alpha$  is small enough. Importantly, the curvaton contribution to the cosmic density fluctuation is inversely proportional to  $\phi_{\text{init}}$  (when  $\phi_{\text{init}}$  is less than  $M_{\text{pl}}$ ). Thus, to make the models viable, upper bounds on  $\phi_{\text{init}}$  is obtained. Similar result is obtained for the natural inflation model.

We also considered the new inflation model. If all the parameters in the inflaton potential (in particular, the  $v$  parameter defined in Eq. (3.9)) are free, the curvaton mechanism can relax the constraint on the new inflation model. However, for some class of the new inflation models, the  $\epsilon$  parameter is supposed to be very small. In such a case, even the curvaton mechanism cannot liberate the constraint. Consequently, for the new inflation model based on  $Z_n$  symmetry proposed in [14, 15], for example, relatively large value of  $n$  is needed.

**Acknowledgment:** We acknowledge the use of CMBFAST [17] package for our numerical calculations. One of the authors (T.T.) is grateful to Fuminobu Takahashi for useful conversation. T.T. would like to thank the Japan Society for Promotion of Science for financial support. The work of T.M. is supported by the Grants-in Aid of the Ministry of Education, Science, Sports, and Culture of Japan No. 15540247.

## References

- [1] A. H. Guth, Phys. Rev. D **23**, 347 (1981);  
K. Sato, Mon. Not. Roy. Astron. Soc. **195**, 467 (1981).
- [2] C. L. Bennett *et al.*, Astrophys. J. Suppl. **148**, 1 (2003) [arXiv:astro-ph/0302207].
- [3] H. V. Peiris *et al.*, Astrophys. J. Suppl. **148**, 213 (2003) [arXiv:astro-ph/0302225].
- [4] A. D. Linde, Phys. Lett. B **129** (1983) 177.
- [5] K. Enqvist and M. S. Sloth, Nucl. Phys. B **626**, 395 (2002) [arXiv:hep-ph/0109214];  
D. H. Lyth and D. Wands, Phys. Lett. B **524**, 5 (2002) [arXiv:hep-ph/0110002];  
T. Moroi and T. Takahashi, Phys. Lett. B **522**, 215 (2001) [Erratum-ibid. B **539**, 303 (2002)] [arXiv:hep-ph/0110096].
- [6] D. Langlois and F. Vernizzi, Phys. Rev. D **70**, 063522 (2004) [arXiv:astro-ph/0403258].
- [7] M. S. Turner, Phys. Rev. D **28**, 1243 (1983).
- [8] T. Moroi and T. Takahashi, Phys. Rev. D **66**, 063501 (2002) [arXiv:hep-ph/0206026].

- [9] S. M. Leach and A. R. Liddle, Phys. Rev. D **68**, 123508 (2003) [arXiv:astro-ph/0306305].
- [10] K. Freese, J. A. Frieman and A. V. Olinto, Phys. Rev. Lett. **65**, 3233 (1990).
- [11] F. C. Adams, J. R. Bond, K. Freese, J. A. Frieman and A. V. Olinto, Phys. Rev. D **47**, 426 (1993) [arXiv:hep-ph/9207245].
- [12] T. Moroi and T. Takahashi, Phys. Lett. B **503**, 376 (2001) [arXiv:hep-ph/0010197].
- [13] L. Verde *et al.*, Astrophys. J. Suppl. **148**, 195 (2003) [arXiv:astro-ph/0302218].
- [14] K. Kumekawa, T. Moroi and T. Yanagida, Prog. Theor. Phys. **92**, 437 (1994) [arXiv:hep-ph/9405337].
- [15] K. I. Izawa and T. Yanagida, Phys. Lett. B **393**, 331 (1997) [arXiv:hep-ph/9608359].
- [16] M. Ibe, K. I. Izawa and T. Yanagida, arXiv:hep-ph/0409203.
- [17] M. Zaldarriaga and U. Seljak, Astrophys. J. **469**, 437 (1996).